Human Pathology (2019) **88**, 48–59

ELSEVIER

Human PATHOLOGY

www.elsevier.com/locate/humpath

Original contribution

# A comparison of adult rhabdomyosarcoma and high-grade neuroendocrine carcinoma of the urinary bladder reveals novel *PPP1R12A* fusions in rhabdomyosarcoma☆,☆☆

**Sounak Gupta MBBS, PhD[a,1], Carlos P. Sosa PhD[a], Farhad Kosari PhD[b], Andrew Folpe MD[a], Kaustubh N. Bhinge PhD[b], Lin Yang PhD[a], Alireza Agahi MD[b], Sarah H. Johnson MS[c], Igor Frank MD[d], Stephen A. Boorjian MD[d], Donna E. Hansel MD, PhD[e], Hikmat A. Al-Ahmadie MD[f], Victor E. Reuter MD[f], George Vasmatzis PhD[b], Rafael E. Jimenez MD[a], Loren Herrera-Hernandez MD[a], John C. Cheville MD[a,*]**

[a]*Department of Laboratory Medicine and Pathology, Mayo Clinic, Rochester, MN 55905*
[b]*Department of Molecular Medicine, Mayo Clinic, Rochester, MN 55905*
[c]*Center for Individualized Medicine, Mayo Clinic, Rochester, MN 55905*
[d]*Department of Urology, Mayo Clinic, Rochester, MN 55905*
[e]*Department of Pathology, University of California at San Diego, CA 92093*
[f]*Department of Pathology, Memorial Sloan Kettering Cancer Center, New York, NY 10065*

Received 11 December 2018; revised 10 March 2019; accepted 14 March 2019

**Keywords:**
Genitourinary;
Urinary bladder;
Rhabdomyosarcoma;
Sarcomatoid carcinoma;
High-grade neuroendocrine carcinoma;
ASCL1;
*PPP1R12A*

**Summary** Some rhabdomyosarcomas and sarcomatoid carcinomas with heterologous rhabdomyosarcomatous elements resemble high-grade neuroendocrine carcinoma, creating a diagnostic difficulty. The purpose of this study was to characterize the overlap of adult genitourinary rhabdomyosarcomas, excluding those occurring at paratesticular sites, with high-grade neuroendocrine carcinoma and identify features helpful in their separation. Seventeen cases of rhabdomyosarcoma (11 from the urinary bladder and 3 each from kidney and prostate) were compared to 10 cases of high-grade neuroendocrine carcinoma from the urinary bladder. These tumors were analyzed by immunohistochemistry for desmin, MyoD1, myogenin, chromogranin, synaptophysin, CD56, TTF1, and ASCL1, and RNA sequencing was performed on 4 cases of bladder rhabdomyosarcoma (2 rhabdomyosarcomas and 2 sarcomatoid-rhabdomyosarcoma) and 10 cases of bladder high-grade neuroendocrine carcinoma. This was compared

☆ Disclosures: none.
☆☆ Preliminary results from this study were presented as an abstract at the 2017 USCAP annual meeting.

* Corresponding author at: Department of Laboratory Medicine and Pathology, Mayo Clinic, 200 First St SW, Rochester, MN 55905.
*E-mail addresses:* guptas1@mskcc.org (S. Gupta), Sosa.Carlos@mayo.edu (C. P. Sosa), Kosari.Farhad@mayo.edu (F. Kosari), folpe.andrew@mayo.edu (A. Folpe), Bhinge.Kaustubh@mayo.edu (K. N. Bhinge), Yang.Lin@mayo.edu (L. Yang), Agahi.Alireza@mayo.edu (A. Agahi), Johnson.Sarah14@mayo.edu (S. H. Johnson), Frank.Igor@mayo.edu (I. Frank), Boorjian.Stephen@mayo.edu (S. A. Boorjian), dhansel@ucsd.edu (D. E. Hansel), alahmadh@mskcc.org (H. A. Al-Ahmadie), reuterv@mskcc.org (V. E. Reuter), vasm@mayo.edu (G. Vasmatzis), Jimenez.Rafael@mayo.edu (R. E. Jimenez), HerreraHernandez.Loren@mayo.edu (L. Herrera-Hernandez), Cheville.John@mayo.edu (J. C. Cheville).
[1] Present institutional affiliation: Department of Pathology, Memorial Sloan Kettering Cancer Center, New York, NY.

https://doi.org/10.1016/j.humpath.2019.03.007

to public data from 414 typical urothelial carcinomas from The Cancer Genome Atlas dataset. Morphologic and immunophenotypic overlap with high-grade neuroendocrine carcinoma was seen in half of the bladder tumors, which included 4 rhabdomyosarcomas and 2 sarcomatoid rhabdomyosarcomas. RNA sequencing confirmed expression of neuroendocrine markers in these cases (2 rhabdomyosarcomas and 2 sarcomatoid rhabdomyosarcomas). Differential neuroendocrine differentiation was highlighted by ASCL1 protein expression only in high-grade neuroendocrine carcinoma. Moreover, both a pure alveolar rhabdomyosarcoma and sarcomatoid rhabdomyosarcoma of the urinary bladder demonstrated a fusion involving *PPP1R12A*. In summary, adult rhabdomyosarcomas of the urinary bladder are molecularly distinct from high-grade neuroendocrine carcinomas based on specific patterns of expression of myogenic and epithelial to mesenchymal transition–related transcription factors as well as the presence of a novel *PPP1R12A* fusion which is seen in a subset of cases.


## 1. Introduction

Adult rhabdomyosarcomas (RMSs) involving the prostate, kidney, and urinary bladder are rare entities and have for the most part been reported as isolated case reports or small series [1-12]. The largest report to date of adult (defined as older than 16 years) sarcomas of these organs, diagnosed over a 25-year span at a referral center, consisted of 74 cases, of which RMSs comprised only 13 cases (renal: 0; bladder: 4; prostate: 9) [13]. Likewise, sarcomatoid carcinomas with heterologous rhabdomyosarcomatous differentiation (S-RMSs) are very rare, with no cases being reported in a recent series of 28 cases of the bladder that were diagnosed over a 13-year span [14].

Recent small studies have reported that adult RMS including tumors of the urinary bladder can resemble small cell carcinoma and express neuroendocrine markers [5,15-17]. This includes the documentation of ultrastructural features of both myogenic and neuroendocrine differentiation characterized by the presence of both bundles of filaments containing abortive Z bands and dense core neurosecretory-type granules in the same cells [5].

Misdiagnosis of RMS of the urinary bladder as small cell carcinoma has significant clinical implications due to the chemosensitive nature of the latter. Indeed, such high-grade neuroendocrine carcinomas (HGNECs) are optimally treated with initial systemic chemotherapy, with recent studies showing significantly improved outcomes following receipt of neoadjuvant chemotherapy followed by definitive local therapy [18-20]. On the other hand, due to the limited number of RMSs identified in the literature, outcomes are poorly defined, with available data suggesting a poor prognosis [17,21]. The clinical implication of confusing S-RMS with HGNEC is less clear, as the optimal treatment approach for S-RMS remains to be defined, although the chemosensitivity of this entity to the agents which target HGNEC has not been well established. The aim of this study was to further characterize adult RMS of the urologic organs and compare these tumors to HGNEC to identify features helpful in their separation.

## 2. Materials and methods

### 2.1. Patient specimens and selection of cases

This study was approved by the institutional review board at Mayo Clinic, Rochester, MN. We identified a total of 17 adult genitourinary RMSs, excluding paratesticular tumors, that were diagnosed between 2002 and 2016. Sixteen cases were evaluated at Mayo Clinic, including 10 received in consultation, and an additional case was evaluated at Memorial Sloan Kettering Cancer Center. Based on preexisting diagnostic criteria including immunophenotypic evidence of myogenic differentiation characterized by expression of desmin, myogenin, and MyoD1, the original diagnosis of RMS was confirmed for 15 cases. We further included 2 additional cases for analyses, 1 originally diagnosed as a leiomyosarcoma which was reclassified following review of renal smooth muscle neoplasms and another case of S-RMS, originally diagnosed as a small cell carcinoma of the bladder, which was identified following review of bladder HGNEC [18,22,23].

### 2.2. Immunohistochemistry

Tumors were immunostained for desmin (Leica, Novocastra, Buffalo Grove, IL; clone DE-R-11, 1:50-1:100), myogenin (Dako, Carpinteria, CA; clone F5D, 1:25-1:50), MyoD1 (Ventana, Tucson, AZ; clone EP212, 1 μg/mL), synaptophysin (Leica, Novocastra, Buffalo Grove, IL; clone 27G12, 1:100-1:200), chromogranin A (Ventana, Tucson, AZ; clone LK2H10, 1 μg/mL), CD56 (Dako, Carpinteria, CA; clone 123C3, 1:50-1:100), TTF1 (Leica, Novocastra, Buffalo Grove, IL; clone SPT24, 1:200), and ASCL1 (BD Pharmingen, San Jose, CA; clone 24B72D11.1, 1:100). Immunohistochemical results were dichotomized into cases with absent expression and those with *positive expression*, defined by staining noted in at least 5% of neoplastic cells. Immunophenotyping of all RMS was performed on representative whole slide sections.

ASCL1 expression in RMSs was compared to 70 patients with HGNEC and 110 patients with typical urothelial carcinomas (UCs) from specimens obtained from patients treated

**Table** Adult genitourinary RMSs: clinicopathological features

| | Kidney | Urinary bladder | Prostate | Summarized data |
|---|---|---|---|---|
| No. of cases | 3 | 11 | 3 | 17 |
| Mean age (y, range) | 58 (54-64) | 60 (19-84) | 44 (23-55) | 57 (19-84) |
| Sex | | | | |
| Male | 2 | 6 | 3 | 11 |
| Female | 1 | 5 | 0 | 6 |
| Histologic subtype | | | | |
| S-RMS | 0 | 5 [a] | 0 | 5 |
| Alveolar | 0 | 4 [b] | 0 | 4 |
| Embryonal | 0 | 1 | 2 | 3 |
| Spindle cell | 3 | 1 | 1 | 5 |
| Morphologic overlap with small cell carcinoma | | | | |
| S-RMS | 0 | 2/5 | 0 | 2/5 |
| Alveolar | 0 | 4/4 | 0 | 4/4 |
| Embryonal | 0 | 0/1 | 0/2 | 0/3 |
| Spindle cell | 0/3 | 0/1 | 0/1 | 0/5 |
| Neuroendocrine differentiation | | | | |
| Synaptophysin | 1/3 | 8/11 | 0/3 | 9/17 |
| Chromogranin | 0/3 | 1/11 | 0/3 | 1/17 |
| CD56 | 3/3 | 10/10 | 2/3 | 15/16 |
| TTF1 | 0/3 | 2/10 | 0/3 | 2/16 |

[a] Documented gene rearrangement in 1 case (*PPP1R12A*, RNAseq).
[b] Documented gene rearrangements in 2 cases include *FOXO1* (n = 1; fluorescence in situ hybridization) and *PPP1R12A* (n = 1; RNAseq).

with radical cystectomy at our institution between 1987 and 2014 [18]. Tissue microarrays, with four 1.0-mm cores representing each HGNEC and typical UC, were immunostained for ASCL1 for this purpose. In addition, whole slide sections of 42 cases of non–urinary bladder RMSs were immunostained for ASCL1 to assess specificity.

### 2.3. RNA sequencing and data extraction from The Cancer Genome Atlas Project

Library preparation and gene expression profiling by RNA sequencing (RNAseq) were performed at the Mayo Clinic Genomic Facility following Institutional Review Board approval using formalin-fixed, paraffin-embedded tissue (2 alveolar RMSs, 2 S-RMSs) as well as archived frozen tissue (10 HGNECs).

All analyses were in the R programing environment. RNA sequence data were mapped on the latest reference genome (HG38) using the STAR aligner and following computational pipeline described in the Genomic Data Commons Web site (https://docs.gdc.cancer.gov/Data/Bioinformatics_Pipelines/Expression_mRNA_Pipeline). This approach allowed us to combine expression count matrices of the RNAseq data generated at Mayo Clinic and The Cancer Genome Atlas data containing 414 typical UCs. Normalized expression matrix for all RNAseq files was generated using edgeR package and then log2 transformed.

Identification of fusion events was by MAP-RSeq pipeline, STAR-Fusion, and FusionInspector, a component of STAR-Fusion (Haas et al (2015) STAR-FUSION, https://github.com/STAR-Fusion/STAR-Fusion, 13 April 2016, date last accessed) [24]. To validate fusion events, RNA was used in reverse-transcription polymerase chain reactions, and the polymerase chain reaction amplicons were inserted into a TA cloning vector. The inserted amplicon was then sequenced by pyrosequencing.

### 2.4. Statistical analysis

Continuous clinicopathological variables were analyzed with frequency counts and percentages. Tests to assess statistical significance were 2-sided, with $P < .05$ considered to be statistically significant.

## 3. Results

### 3.1. Clinicopathological features

Clinicopathological features of the 17 cases of RMS and S-RMS are provided in the Table, including 3 renal, 11 bladder, and 3 prostatic tumors. Mean age at diagnosis was 57 years (range, 19-84) (renal: 58 years, range, 54-64; urinary bladder: 60 years, range, 19-84; prostate: 44 years, range, 23-55). No sex predilection was identified in the bladder tumors.

The 5 cases classified as S-RMS had a concurrent UC component (in situ, n = 2 and UC not otherwise specified, n = 3), and all tumors were positive for cytokeratin. Six cases

of pure RMS of the urinary bladder included alveolar (n = 4), embryonal (n = 1), and spindle cell (n = 1) subtypes. Of the renal and prostate RMS, none were associated with a sarcomatoid carcinoma component and were classified as spindle cell (n = 4) and embryonal subtypes (n = 2). None of the renal or prostate RMSs had appreciable morphologic overlap with HGNEC. However, 4 cases of bladder RMS (all pure alveolar) and two S-RMSs exhibited significant morphologic overlap with small cell carcinomas (Fig. 1).

Clinical follow-up of at least 6 months was available for 3 patients with bladder RMS and 2 patients with bladder S-RMS. Four of these patients had tumors which exhibited morphologic/immunophenotypic overlap with HGNEC. The first, a 74-year-old man with S-RMS, died of disease-related complications including metastasis to the brain at 10 months. The second patient, a 69-year-old man with S-RMS, developed bone metastases at 6 months of follow-up. The third, a 72-year-old man with a pure RMS, died of disease at 110 months. This included widely metastatic disease (brain and lung). The fourth patient, a 19-year-old man with a *FOXO1* rearranged alveolar RMS, was alive with a biopsy-proven left supraclavicular lymph node metastasis at 27 months.

Finally, a 37-year-old woman with an embryonal RMS that did not exhibit morphologic/immunophenotypic overlap with HGNEC was alive without disease at 158 months following initial management with a partial cystectomy.

### 3.2. Immunohistochemistry

Immunohistochemistry was performed to assess expression of chromogranin, synaptophysin, CD56, and TTF1. Although a combination of desmin, MyoD1, and myogenin confirmed myogenic differentiation for pure RMS or S-RMS, aberrant expression of neuroendocrine markers was relatively common, as we have previously reported (Fig. 2, Table) [15]. CD56 demonstrated the least specificity, being detected in 15 (of 16, 94%) RMSs. This was followed by synaptophysin (9 of 17, 53%), whereas the expression of chromogranin (1 of 17, 6%) and TTF1 (2 of 16, 13%) was infrequent. The morphologic overlap with small cell carcinoma in 6 cases of bladder RMS and S-RMS, coupled with the expression of neuroendocrine markers (CD56: 5 of 5, 100%; synaptophysin: 5 of 6, 83%; TTF1: 2 of 5, 40%; chromogranin: 1 of 6, 17%), highlights the diagnostic pitfall of misclassifying these cases as small cell carcinomas.

### 3.3. Gene expression analysis

RNAseq analysis was performed on 4 cases of bladder RMS (pure alveolar: 2 and S-RMS: 2) and 10 cases of HGNEC. This analysis was compared to 414 typical UCs from the publicly available The Cancer Genome Atlas database. The dataset was validated by assaying for a gene expression signature characteristic of UC (not shown), which

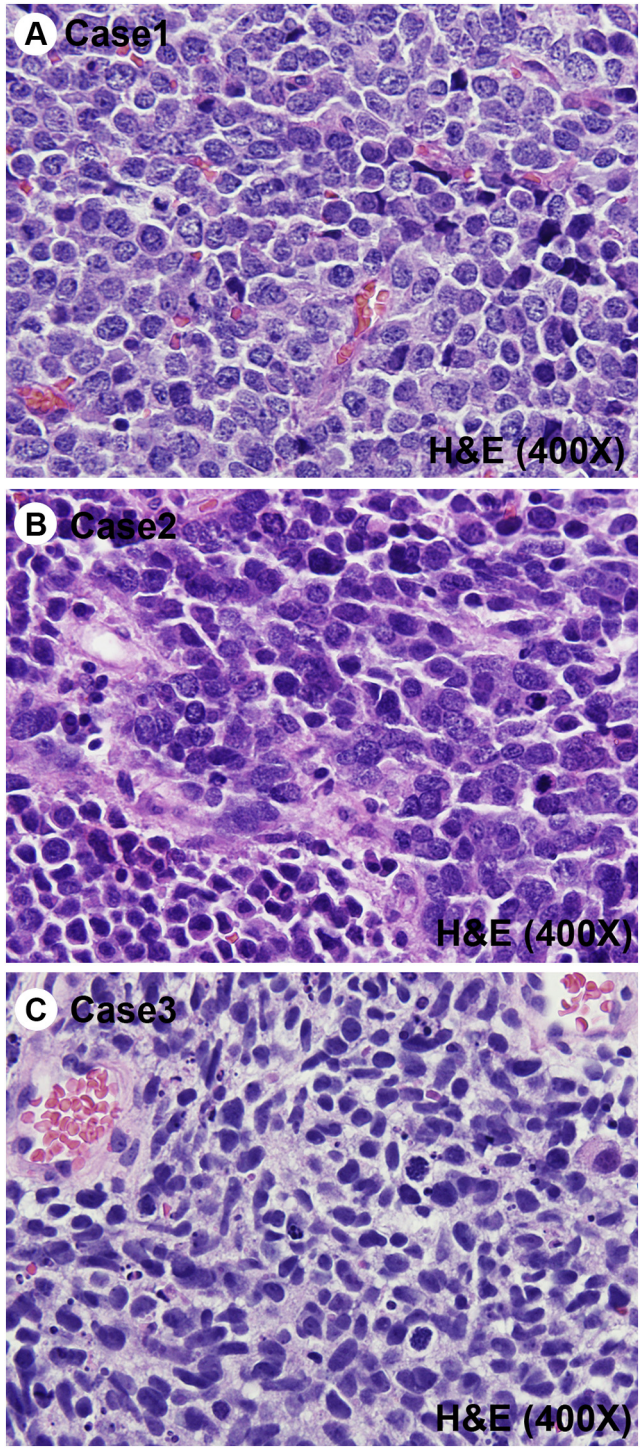


**Fig. 1** Adult genitourinary RMS: histopathology. Representative hematoxylin and eosin (H&E)–stained images of pure RMSs of the urinary bladder (A and B; original magnification ×400) and a S-RMS showing morphologic overlap with small cell carcinoma (C; ×400).

was not enriched in the other tumor types (UC versus HGNEC, $P < .005$), including *keratin 7* (*KRT7*), *keratin 19* (*KRT19*), *uroplakin 2* (*UPK2*), *claudin 4* (*CLDN4*), *GATA binding protein 3* (*GATA3*), *CD44 molecule* (*CD44*), *tumor protein p63* (*TP63*), and *cyclin D1* (*CCND1*).

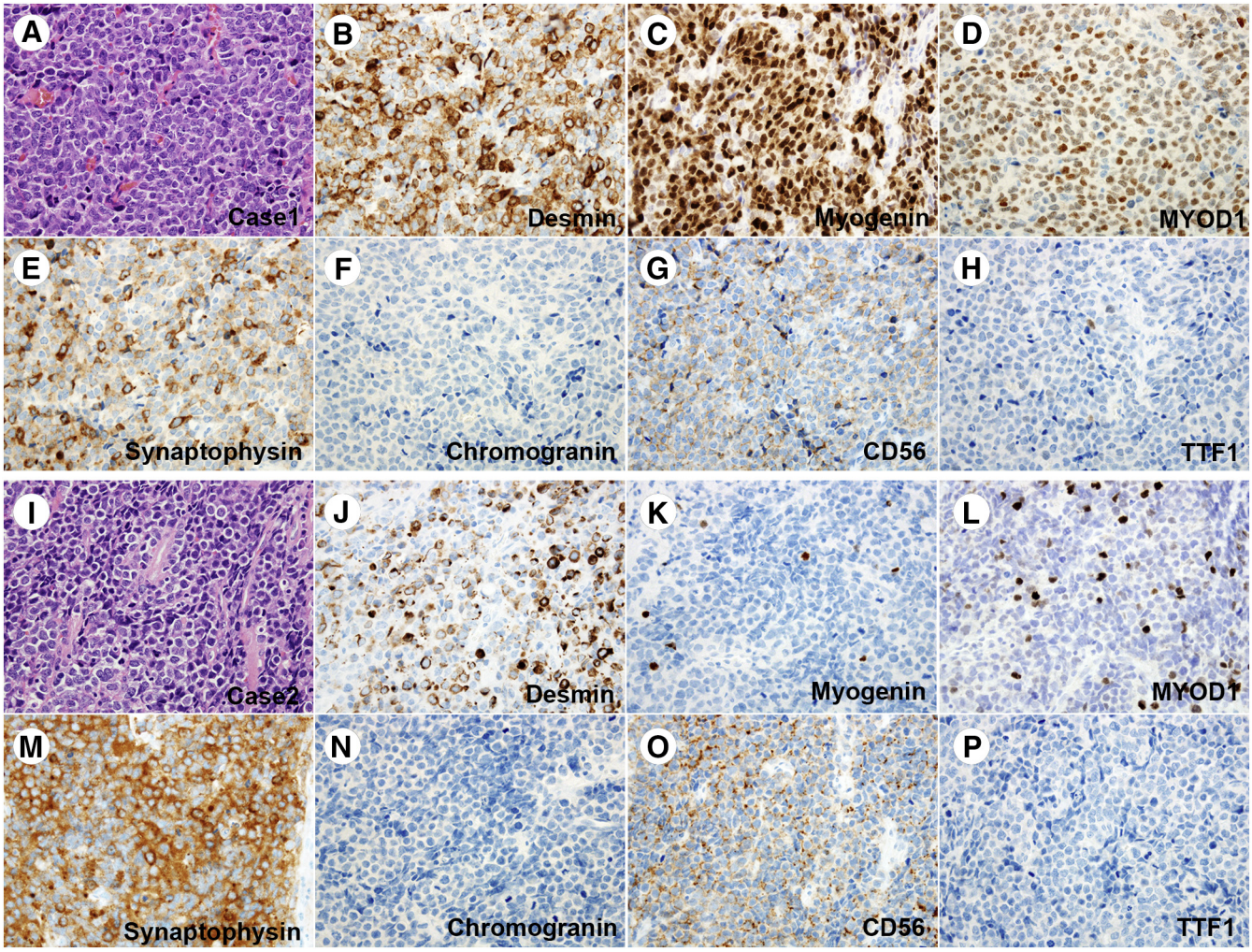


**Fig. 2** Adult genitourinary RMS: immunohistochemistry. Representative images detailing the immunophenotype of RMSs of the urinary bladder, which demonstrate morphologic overlap with small cell carcinoma (case 1: A-H, case 2: I-P, ×200). H&E-stained images (A and I); immunohistochemistry for desmin (B and J), myogenin (C and K), MyoD1 (D and L), synaptophysin (E and M), chromogranin (F and N), CD56 (G and O), and TTF1 (H and P) is shown.

Assessment of gene expression for markers of neuroendocrine differentiation mirrored our immunohistochemical results, with increased expression of *synaptophysin* (*SYP*), *chromogranin A* (*CHGA*), *chromogranin B* (*CHGB*), and *neural cell adhesion molecule 1* (*NCAM1*, which encodes for the CD56 protein) showing high levels of expression in both HGNEC and RMS/S-RMS, with no expression detected in UC (Fig. 3). Less common genes associated with neuroendocrine differentiation such as *proprotein convertase subtilisin/kexin type 1* (*PCSK1*) and *secretogranin II* (*SCG2*) showed a similar pattern as well. However, at the gene expression level, *insulinoma-associated 1* (*INSM1*) and *achaete-scute family bHLH transcription factor 1* (*ASCL1*) did not show significant changes. Statistical analysis for RMS, however, was limited by the restricted number of cases analyzed (n = 4).

Furthermore, gene expression of transcription factors that drive both myogenic differentiation (Fig. 4) and epithelial to mesenchymal transitions (Fig. 5) was assessed [14,21]. As expected, myogenic transcription factors including *myogenin* and *myogenic differentiation 1* (*MYOD1*) showed a significant increase in expression in RMS/S-RMS compared to cases of UC and HGNEC, consistent with results of immunohistochemistry. Meanwhile, expression of the myogenic transcriptional regulator *forkhead box O1* (*FOXO1*) was similar in RMS, whereas *paired box 3* (*Pax3*), *paired box 7*

**Fig. 3** Adult genitourinary RMS: neuroendocrine gene expression. Relative gene expression (log2) for UCs (n = 414), HGNECs (n = 10), S-RMSs (n = 2), and pure RMSs (n = 2) for PCSK1 (A), SCG2 (B), NCAM1 (C), CHGB (D), CHGA (E), SYP (F), ASCL1 (G), and INSM1 (H) is shown.

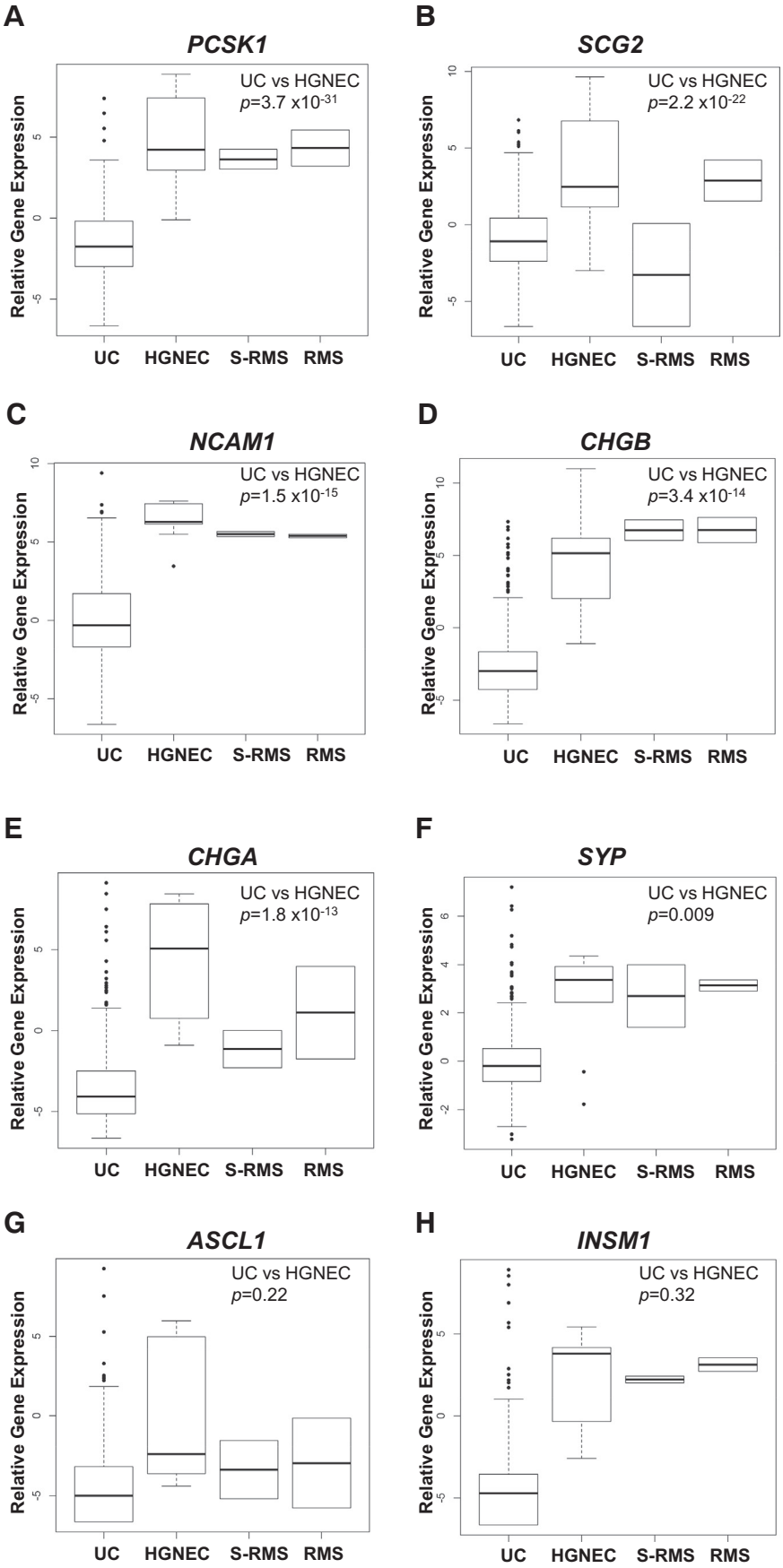
A
PCSK1
UC vs HGNEC
p=3.7 x10-31
Relative Gene Expression
UC HGNEC S-RMS RMS
B
SCG2
UC vs HGNEC
p=2.2 x10-22
Relative Gene Expression
UC HGNEC S-RMS RMS
C
NCAM1
UC vs HGNEC
p=1.5 x10-15
Relative Gene Expression
UC HGNEC S-RMS RMS
D
CHGB
UC vs HGNEC
p=3.4 x10-14
Relative Gene Expression
UC HGNEC S-RMS RMS
E
CHGA
UC vs HGNEC
p=1.8 x10-13
Relative Gene Expression
UC HGNEC S-RMS RMS
F
SYP
UC vs HGNEC
p=0.009
Relative Gene Expression
UC HGNEC S-RMS RMS
G
ASCL1
UC vs HGNEC
p=0.22
Relative Gene Expression
UC HGNEC S-RMS RMS
H
INSM1
UC vs HGNEC
p=0.32
Relative Gene Expression
UC HGNEC S-RMS RMS

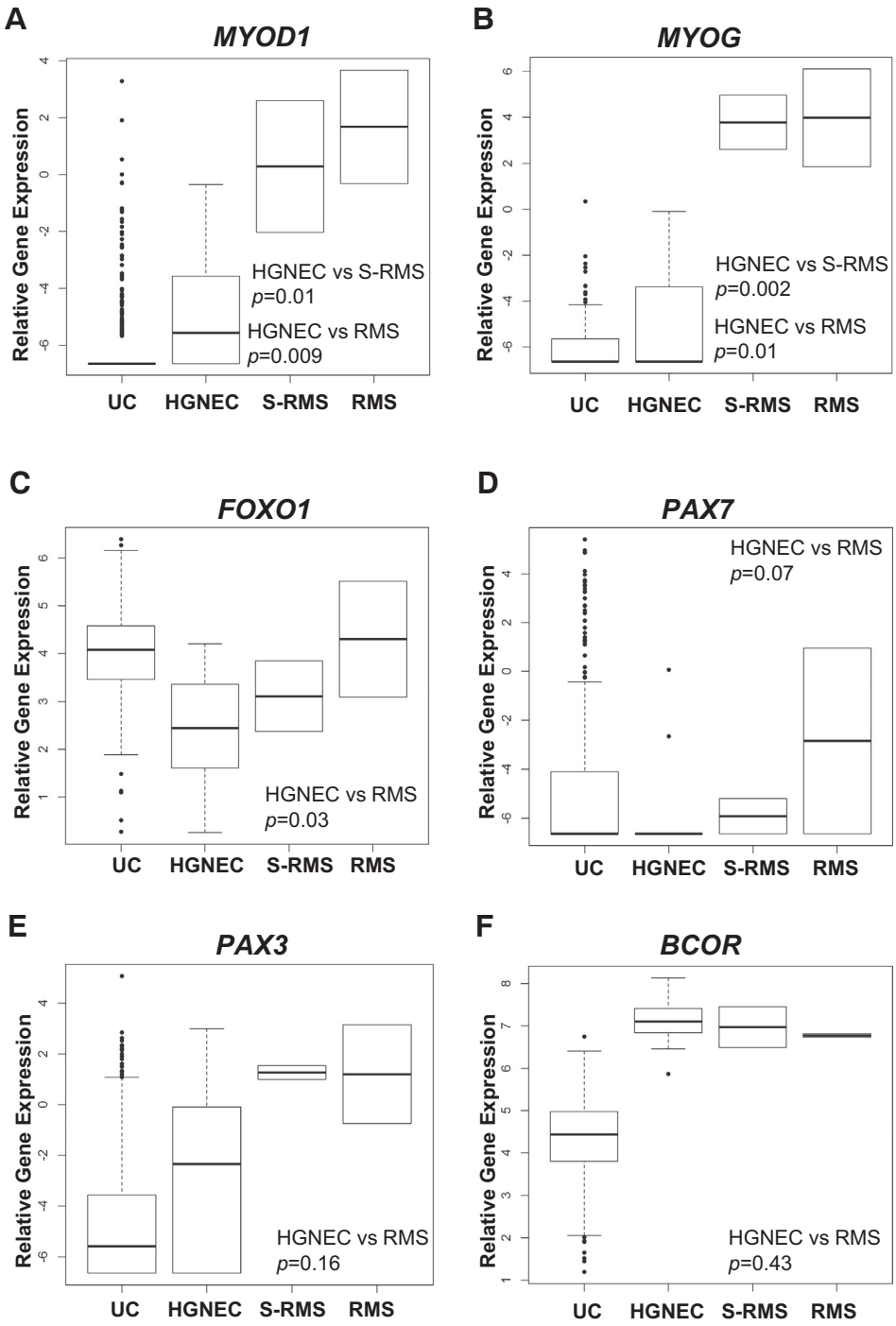


**Fig. 4** Gene expression of transcriptional regulators of myogenesis. Relative gene expression ($log_2$) for UCs (n = 414), HGNECs (n = 10), S-RMSs (n = 2), and pure RMSs (n = 2) for *MYOD1* (A) and *Myogenin* (B), *FOXO1* (C), *PAX7* (D), *PAX3* (E), and *BCOR* (F) is shown.

(*Pax7*), and *BCL6 corepressor* (*BCOR*) did not show a difference in expression. The transcription factors *zinc finger E-box binding homeobox 1* and *2 (ZEB1/ZEB2*) that are known to drive epithelial to mesenchymal transition showed highest expression in S-RMS compared to UC, HGNEC, and pure RMS. Other regulators such as *snail family transcriptional repressor 2* (*SNAI2*) and *twist family bHLH transcription factor 1* (*TWIST1*) did not exhibit differential expression.

### 3.4. Immunohistochemistry, ASCL1

ASCL1 expression has been found to be a specific marker of neuroendocrine differentiation in several tumor types and in our series of lung adenocarcinomas with neuroendocrine differentiation [25,26]. Herein, ASCL1 immunohistochemistry showed a lower sensitivity for the detection of HGNEC relative to other neuroendocrine markers (present in 34 of

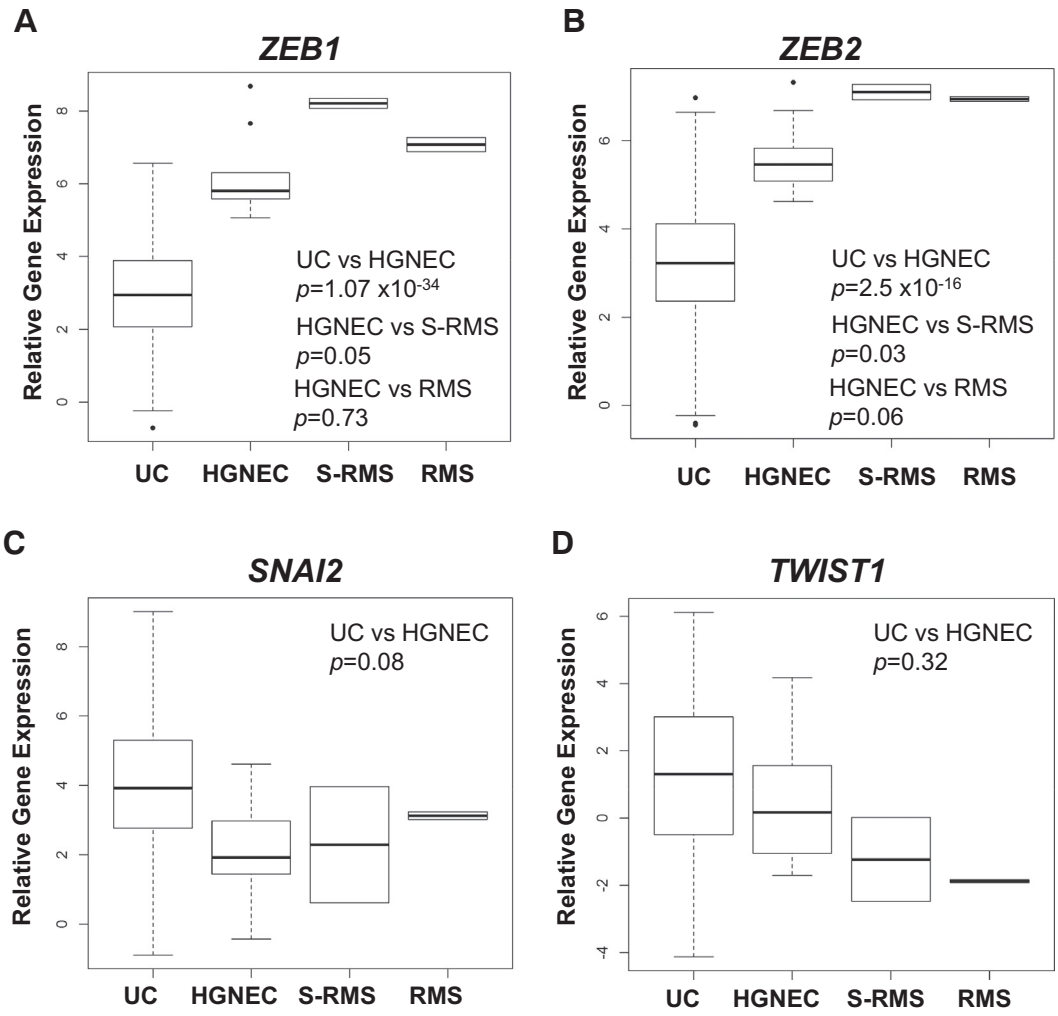


**Fig. 5** Gene expression of transcriptional regulators of epithelial to mesenchymal transition. Relative gene expression ($log_2$) for UCs (n = 414), HGNECs (n = 10), S-RMSs (n = 2), and pure RMSs (n = 2) for *ZEB1* (A) and *ZEB2* (B), *SNAI2* (C), and *TWIST1* (D) is shown.

70 cases; 49%) (Fig. 6, Supplementary Table 1). However, ASCL1 immunohistochemical positivity was highly specific for HGNEC, as expression was not seen in typical UCs (0 of 110 cases), pure RMSs (0 of 7 cases), and S-RMSs (0 of 2 cases). To assess specificity, 42 cases of non–urinary bladder RMSs (16 embryonal, 1 spindle cell, 8 pleomorphic, and 17 alveolar) were tested for ASCL1 expression by immunohistochemistry, and all cases were negative.

### 3.5. Gene rearrangements

RNAseq analysis for the 4 cases of RMS/S-RMS did not reveal any structural rearrangements for genes commonly rearranged in alveolar RMS, such as *Pax3*, *Pax7*, and *FOXO1*. Interestingly, we identified fusions involving genes at the 12q21.1 to 12q21.31 locus for 1 case each of pure RMS and S-RMS (Fig. 7A). The specific events included a structural rearrangement between exon 2 of *protein phosphatase 1 regulatory subunit 12A* (*PPP1R12A*) and exon 2 of *lin-7 homolog A* (*LIN7A*) in the first case (Fig. 7B and C). In the second case, a fusion between exon 10 of *PPP1R12A* and exon 4 of *protein tyrosine phosphatase, receptor type Q* (*PTPRQ*) was documented (Fig. 7D and E).

## 4. Discussion

Adult genitourinary RMS and S-RMS are rare. A total of 12 cases of pure RMS and 5 cases of S-RMS were identified in our study over a 14-year period, with the majority (11 cases) involving the urinary bladder. Similar to prior studies that documented a striking morphologic overlap with HGNEC, we identified 6 such cases, all involving the urinary bladder. The RMSs seen in the kidney and prostate were classified as embryonal or spindled subtypes and bore no morphologic resemblance to small cell carcinoma. Prior studies of pure RMS of the bladder have documented a neuroendocrine phenotype characterized by the expression of a

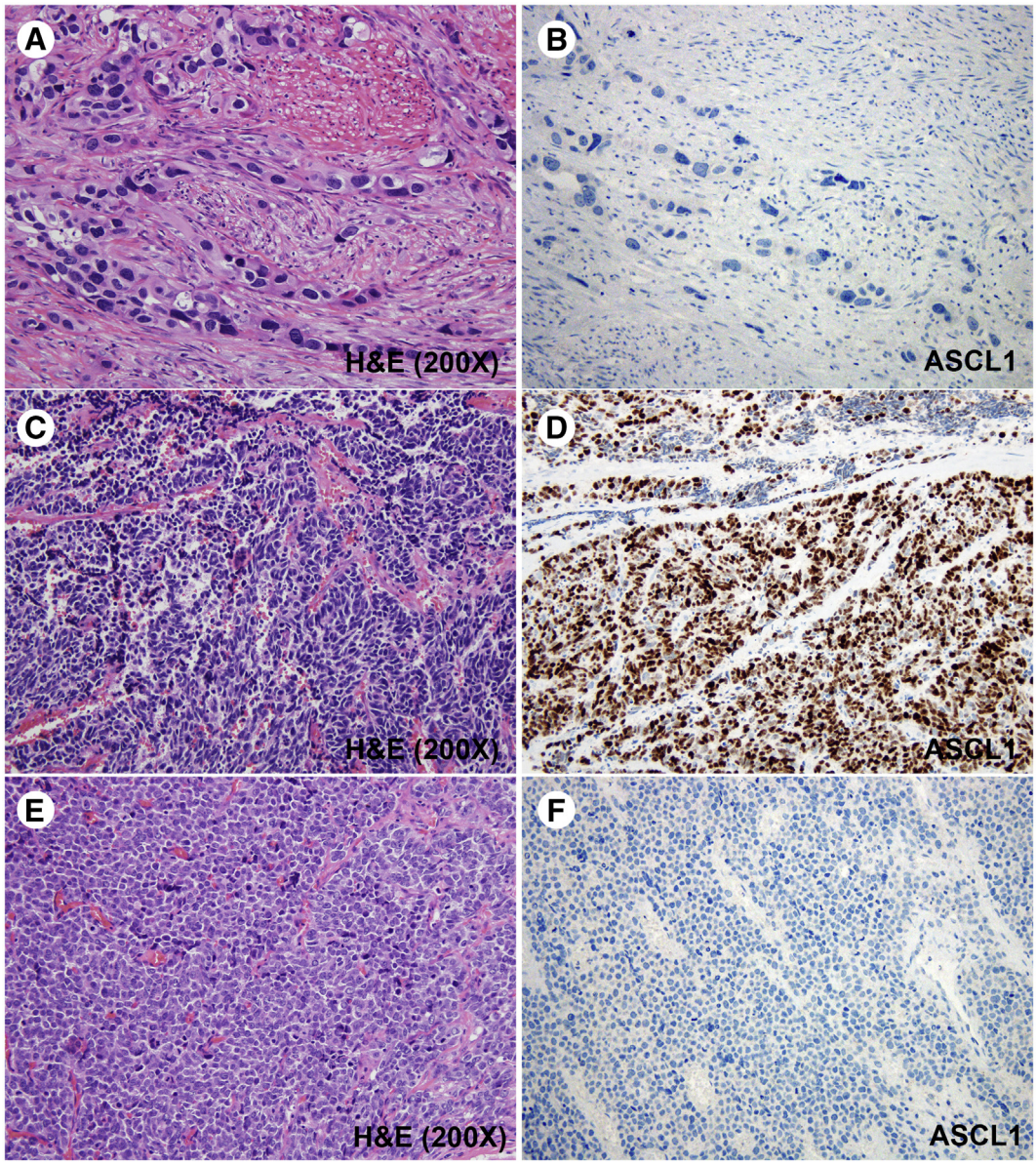


**Fig. 6** Adult genitourinary RMS: immunohistochemistry, ASCL1. Representative H&E-stained images and corresponding ASCL1 expression in a typical UC (A and B, ×200), HGNEC (C and D, ×200), and pure RMS (E and F, ×200) are shown.

combination of synaptophysin, chromogranin, and neuron-specific enolase in 1 case reported by Eusebi et al, in 3 (of 4) cases reported by Paner et al, and in 1 case reported by Bing et al [5,16,17]. Similar expression of neuroendocrine markers in RMS occurring as heterologous elements in S-RMS of the bladder was reported in 2 cases by Bing et al [16].

Herein, we report a series of 6 cases of pure RMS and 5 S-RMSs of the bladder. All 11 cases showed expression of neuroendocrine markers, with 6 of these cases showing significant morphologic overlap with small cell carcinoma, similar to the reports of Eusebi et al, Paner et al, and Bing et al [5,16,17]. Also, consistent with prior studies primarily focused on head and neck alveolar RMS, CD56 was almost

**Fig. 7** Confirmation of *PPP1R12A* gene fusion in pure RMSs of the bladder. A, A schematic representation of the *PPP1R12A-LIN7A* and *PPP1R12A-PTPRQ* structural variants. Pyrosequencing traces demonstrate the breakpoint between exon 2 of *PPP1R12A* and exon 2 of *LIN7A* on forward (B) and reverse (C) traces. Similarly, the breakpoint between exon 10 of *PPP1R12A* and exon 4 of *PTPRQ* has been shown on both forward (D) and reverse (E) traces.

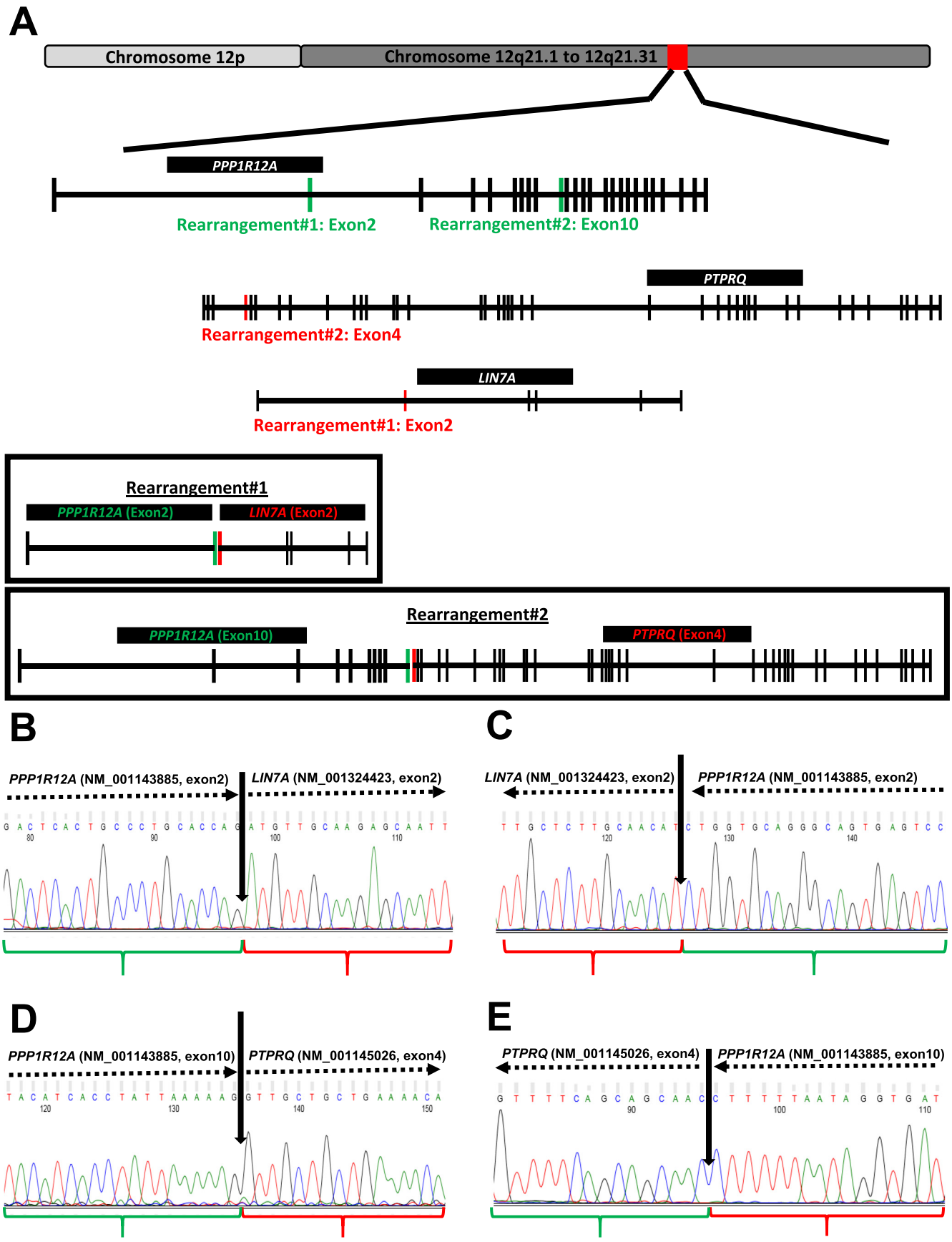
A
Chromosome 12p
Chromosome 12q21.1 to 12q21.31
PPP1R12A
Rearrangement#1: Exon2
Rearrangement#2: Exon10
PTPRQ
Rearrangement#2: Exon4
LIN7A
Rearrangement#1: Exon2
Rearrangement#1
PPP1R12A (Exon2)
LIN7A (Exon2)
Rearrangement#2
PPP1R12A (Exon10)
PTPRQ (Exon4)
B
PPP1R12A (NM_001143885, exon2)
LIN7A (NM_001324423, exon2)
C
LIN7A (NM_001324423, exon2)
PPP1R12A (NM_001143885, exon2)
D
PPP1R12A (NM_001143885, exon10)
PTPRQ (NM_001145026, exon4)
E
PTPRQ (NM_001145026, exon4)
PPP1R12A (NM_001143885, exon10)

ubiquitously expressed in all but one of our cases, and half the cases expressed one of the more specific neuroendocrine markers (synaptophysin in 9; chromogranin in 1) compared to our reported rate of 30%-40% for synaptophysin/chromogranin in head and neck alveolar RMS [15]. Our prior study of 79 HGNECs compared to 122 stage-matched UCs of the bladder had shown a high diagnostic specificity of chromogranin (100%), synaptophysin (98%), TTF1 (97%), and CD56 (96%) in differentiating HGNEC from UC [18]. In this context, this is a noteworthy diagnostic pitfall, as 6 cases of RMS/S-RMS had a significant morphologic overlap with HGNEC. This is highlighted by the identification of a case of S-RMS in our series, originally diagnosed as small cell carcinoma of the urinary bladder [18].

Furthermore, the neuroendocrine immunophenotype was concordant with the underlying gene expression signature, as *SYP*, *CHGA*, *CHGB*, and *NCAM1* expression was roughly equivalent in both HGNEC and RMS/S-RMS. A similar pattern was seen for *PCSK1* and *SCG2*, as well.

*ASCL1* is a basic helix-loop-helix transcriptional factor that plays a major role in differentiation during neurogenesis, and previous studies have showed that its expression defined a subset of lung adenocarcinomas with neuroendocrine differentiation [25,26]. Although *ASCL1* mRNA expression did not reliably discriminate between HGNEC and UC, our results indicate that immunohistochemical detection of the corresponding protein has a high specificity for HGNEC because it was not detected in any of 110 cases of UC, 9 genitourinary RMSs, or 42 non-bladder RMSs that were tested. Although ASCL-1 is highly specific for neuroendocrine differentiation in the carcinomas, its clinical utility is limited by the lower sensitivity of this marker.

A pure alveolar RMS and a S-RMS profiled by RNAseq that resembled HGNEC had novel fusions involving *PPP1R12A* at the 12q21.1 to 12q21.31 locus. *PPP1R12A*, also known as the myosin-binding subunit of myosin phosphatase, plays an important role in the regulation of actin-myosin contractile dynamics [27]. In a physiologic context, this active protein complex dephosphorylates the myosin light chain kinase. This inhibits the interaction of actin and myosin subunits and consequently smooth muscle contraction. Both identified structural rearrangements disrupt the full-length *PPP1R12A* gene, potentially leading to the interaction of actin and myosin subunits. Prior studies looking at active phosphatases that were expressed at high baseline levels in primary RMS had identified *PPP1R12A* as a candidate target gene; however, to the best of our knowledge, gene fusions involving *PPP1R12A* have not been previously described in RMS in the current English-language literature [28,29]. Specifically, global fusion transcriptome profiling for recurrent chromosomal rearrangements in RMS in at least 2 studies have not revealed any structural variants involving the *PPP1R12A* gene, and similar datasets are not available for bladder RMS in the reviewed English-language literature [21,30]. Additional studies examining larger numbers of alveolar RMS of the urinary bladder are required to determine the significance of this fusion and its potential role in diagnosis. Furthermore, the functional role of this fusion product needs to be determined, as does its relationship to neuroendocrine differentiation.

Our current understanding of transcriptional regulation of mammalian myogenesis suggests that *PAX7* promotes initial lineage specification followed by lineage commitment by *MYOD1* and terminal differentiation by *myogenin* [31]. All the RMSs/S-RMSs profiled by RNAseq showed a gene expression profile that had high levels of the myogenic transcription factors *myogenin* and *MyoD1*, and this was compatible with the observed immunostaining profile for these cases. Epithelial to mesenchymal transition occurs during embryologic development, and similar pathways play an important role in oncogenesis. This involves the upregulation of key transcriptional factors such as *SNAI2*, *ZEB1*/*ZEB2*, and *TWIST1* [14,32]. Transcription factors such as *ZEB1* and *ZEB2* were upregulated in both HGNEC and RMS/S-RMS, relative to UC, with significantly higher levels of *ZEB2* expression being noted in S-RMS. This overall pattern of gene expression highlights multiple pathways related to myogenesis as well as epithelial to mesenchymal transition, which influence the genetic makeup of RMS/S-RMS and contribute to its unique phenotype.

Prior work by Eusebi et al had suggested that bladder RMS in adults is similar to HGNEC [5]. Our study supports the findings of Paner et al in interpreting these bladder RMSs as distinct from HGNECs based on a lack of immunophenotypic evidence of epithelial differentiation and gene expression studies that show expression of a larger number of genes involved in myogenic differentiation [17].

In summary, adult RMSs/S-RMSs of the urinary bladder showed morphologic and immunophenotypic overlap with HGNECs, and neuroendocrine differentiation in the former is supported by gene expression analyses. These tumors, however, have an altered genetic makeup that can be attributed to increased expression of myogenic transcription factors as well as a unique gene fusion event involving *PPP1R12A* in a subset of cases. Practically, in cases of suspected small cell carcinoma of the urinary bladder that express one or more neuroendocrine markers but lack unequivocal keratin staining, application of desmin, myoD1, and myogenin is necessary to exclude RMS. The role of *PPP1R12A* fusion events in the diagnosis of RMS of the urinary bladder is yet to be defined.

## Supplementary data

Supplementary data to this article can be found online at https://doi.org/10.1016/j.humpath.2019.03.007.

## Acknowledgment

The authors have no conflicts of interest or funding to disclose. S. G., C. P. S., F. K., A. F., K. N. B., L. Y., A. A.,

S. H. J., I. F., S. A. B., D. E. H., H. A. A., V. E. R., G. V., R. E. J., L. H. H., and J. C. C. performed the research; S. G., F. K., and J. C. C. designed the research study; S. G., C. P. S., F. K., and J. C. C. analyzed the data; S. G. and J. C. C. wrote the paper. The authors would like to thank Brian Haas from the Broad Institute of MIT and Harvard for his assistance with STAR-Fusion and FusionInspector. The authors would like to thank Janis L. Donovan for administrative assistance.

## References

[1] Ahlering TE, Weintraub P, Skinner DG. Management of adult sarcomas of the bladder and prostate. J Urol 1988;140:1397-9.
[2] Aydoganli L, Tarhan F, Atan A, Akalin Z, Yildiz M. Rhabdomyosarcoma of the urinary bladder in an adult. Int Urol Nephrol 1993;25:159-61.
[3] Chen KW, Wu FM, Lee VK, Esuvaranathan K. Embryonal rhabdomyosarcoma of the adult urinary bladder: a rare case report of misclassification as inflammatory myofibroblastic tumor. Case Rep Surg 2015;2015:510508.
[4] Childs L, Hull D, Bostwick DG. Adult urinary bladder rhabdomyosarcoma. Urology 2008;72:948.e941-3.
[5] Eusebi V, Damiani S, Pasquinelli G, Lorenzini P, Reuter VE, Rosai J. Small cell neuroendocrine carcinoma with skeletal muscle differentiation: report of three cases. Am J Surg Pathol 2000;24:223-30.
[6] Kerr KM, Grigor KM, Tolley DA. Rhabdomyosarcoma of the adult urinary bladder after radiotherapy for carcinoma. Clin Oncol (R Coll Radiol) 1989;1:115-6.
[7] Kunze E, Theuring F, Kruger G. Primary mesenchymal tumors of the urinary bladder. A histological and immunohistochemical study of 30 cases. Pathol Res Pract 1994;190:311-32.
[8] Lambert I, Debiec-Rychter M, Dubin M, Sciot R. Solid alveolar rhabdomyosarcoma originating from the urinary bladder in an adult. Diagnostic value of molecular genetics. Histopathology 2004;44:508-10.
[9] Lauro S, Lalle M, Scucchi L, Vecchione A. Rhabdomyosarcoma of the urinary bladder in an elderly patient. Anticancer Res 1995;15:627-9.
[10] Taylor RE, Busuttil A. Case report: adult rhabdomyosarcoma of bladder, complete response to radiation therapy. J Urol 1989;142:1321-2.
[11] Zarabi CM, Huntrakoon M, Fine KD. Disseminated rhabdomyosarcoma of the urinary bladder in an adult. South Med J 1987;80:526-9.
[12] Ziari M, Sonpavde G, Shen S, Zhai J, Teh BS, Lerner SP. Patients with unusual bladder malignancies and a rare cause of splenomegaly. Case 2. Rhabdomyosarcoma of the urinary bladder in an adult. J Clin Oncol 2005;23:4459-60.
[13] Dotan ZA, Tal R, Golijanin D, et al. Adult genitourinary sarcoma: the 25-year Memorial Sloan-Kettering experience. J Urol 2006;176:2033-8 [discussion 2038-2039].
[14] Sanfrancesco J, McKenney JK, Leivo MZ, Gupta S, Elson P, Hansel DE. Sarcomatoid urothelial carcinoma of the bladder: analysis of 28 cases with emphasis on clinicopathologic features and markers of epithelial-to-mesenchymal transition. Arch Pathol Lab Med 2016;140:543-51.
[15] Bahrami A, Gown AM, Baird GS, Hicks MJ, Folpe AL. Aberrant expression of epithelial and neuroendocrine markers in alveolar rhabdomyosarcoma: a potentially serious diagnostic pitfall. Mod Pathol 2008;21:795-806.
[16] Bing Z, Zhang PJ. Adult urinary bladder tumors with rhabdomyosarcomatous differentiation: clinical, pathological and immunohistochemical studies. Diagn Pathol 2011;6:66.
[17] Paner GP, McKenney JK, Epstein JI, Amin MB. Rhabdomyosarcoma of the urinary bladder in adults: predilection for alveolar morphology with anaplasia and significant morphologic overlap with small cell carcinoma. Am J Surg Pathol 2008;32:1022-8.
[18] Gupta S, Thompson RH, Boorjian SA, et al. High grade neuroendocrine carcinoma of the urinary bladder treated by radical cystectomy: a series of small cell, mixed neuroendocrine and large cell neuroendocrine carcinoma. Pathology 2015;47:533-42.
[19] Kaushik D, Frank I, Boorjian SA, et al. Long-term results of radical cystectomy and role of adjuvant chemotherapy for small cell carcinoma of the bladder. Int J Urol 2015;22:549-54.
[20] Siefker-Radtke AO, Dinney CP, Abrahams NA, et al. Evidence supporting preoperative chemotherapy for small cell carcinoma of the bladder: a retrospective review of the M. D. Anderson cancer experience. J Urol 2004;172:481-4.
[21] Shern JF, Chen L, Chmielecki J, et al. Comprehensive genomic analysis of rhabdomyosarcoma reveals a landscape of alterations affecting a common genetic axis in fusion-positive and fusion-negative tumors. Cancer Discov 2014;4:216-31.
[22] Gupta S, Jimenez RE, Folpe AL, Cheville JC. Renal leiomyoma and leiomyosarcoma: a study of 57 cases. Am J Surg Pathol 2016;40:1557-63.
[23] Gupta S, Sahu D, Bomalaski JS, et al. Argininosuccinate synthetase-1 (ASS1) loss in high-grade neuroendocrine carcinomas of the urinary bladder: implications for targeted therapy with ADI-PEG 20. Endocr Pathol 2018;29:236-41.
[24] Kalari KR, Nair AA, Bhavsar JD, et al. MAP-RSeq: Mayo analysis pipeline for RNA sequencing. BMC Bioinformatics 2014;15:224.
[25] Bhinge K, Yang L, Terra S, et al. EGFR mediates activation of RET in lung adenocarcinoma with neuroendocrine differentiation characterized by ASCL1 expression. Oncotarget 2017;8:27155-65.
[26] Kosari F, Ida CM, Aubry MC, et al. ASCL1 and RET expression defines a clinically relevant subgroup of lung adenocarcinoma characterized by neuroendocrine differentiation. Oncogene 2014;33:3776-83.
[27] Velasco G, Armstrong C, Morrice N, Frame S, Cohen P. Phosphorylation of the regulatory subunit of smooth muscle protein phosphatase 1M at Thr850 induces its dissociation from myosin. FEBS Lett 2002;527:101-4.
[28] Hu K, Lee C, Qiu D, et al. Small interfering RNA library screen of human kinases and phosphatases identifies polo-like kinase 1 as a promising new target for the treatment of pediatric rhabdomyosarcomas. Mol Cancer Ther 2009;8:3024-35.
[29] Romualdi C, De Pitta C, Tombolan L, et al. Defining the gene expression signature of rhabdomyosarcoma by meta-analysis. BMC Genomics 2006;7:287.
[30] Xie Z, Babiceanu M, Kumar S, et al. Fusion transcriptome profiling provides insights into alveolar rhabdomyosarcoma. Proc Natl Acad Sci U S A 2016;113:13126-31.
[31] Charville GW, Varma S, Forgo E, et al. PAX7 expression in rhabdomyosarcoma, related soft tissue tumors, and small round blue cell neoplasms. Am J Surg Pathol 2016;40:1305-15.
[32] Lamouille S, Xu J, Derynck R. Molecular mechanisms of epithelial-mesenchymal transition. Nat Rev Mol Cell Biol 2014;15:178-96.